Chall. Nano Micro Scale Sci. Tech., 10(1): 21-26, Winter and Spring 2022
DOI: 10.22111/CNMST.2022.42471.1227

ORIGINAL RESEARCH PAPER

Electroosmotic motion of aqueous solution containing Mg^{++} inside a silicon nanochannel using Molecular Dynamics simulation

Mohammad Kalteh , M.H. Shabani*

Department of Mechanical Engineering, University of Guilan, Iran

Received 23 May 2022; revised 15 September 2022; accepted 13 November 2022; available online 12 March 2023

ABSTRACT: Electroosmotic motion of water and Na, Cl and Mg ions within a silicon nanochannel which is applicable in drug delivery and lab-on-a-chip systems is studied in this article using Molecular Dynamics. How reverse flow takes place in presence of Mg^{++} has not been thoroughly studied in this field, which is done in this paper. The nanochannel is considered as two parallel surfaces made up of silicon. The ultimate aim here is to evaluate the relation between the electroosmotic flow and channel's surface charge density. Variations in the velocity profile and ion concentration for different surface charge densities are also demonstrated. In low surface charge densities and within the Debye–Hückel flow regime, any increase in surface charge density contributes to an increase in electroosmotic velocity. Having reached to intermediate flow regime boundaries, the flow loses velocity with more surface charge density. This leads to the point that reverse flow can happen due to extremely high surface charge densities, where more surface charge density means more reversed flow velocity. Furthermore, addition of Mg^{++} ion to water-NaCl solution results in up to 31 percent increase in average velocity of the electroosmotic motion with fixed charge density.

KEYWORDS: *Aqueous solution; Electroosmotic motion; Mg ions; Molecular Dynamics simulation; Nanochannel; Surface charge density*

INTRODUCTION

Electroosmosis is the flow of ionized liquid by an applied electric field. This flow is the result of Electrical Double Layer (EDL) formation which is made up of Stern and diffuse sublayers. When a static charged surface is placed in the vicinity of an ionized fluid, like-ions are repelled from and opposite-ions are attracted to the surface. As a result, an EDL with positive or negative charge is formed near the surface. Imposing an external electric field, ions inside the diffuse sublayer start moving and atoms of the fluid follow this movement. In fact, the created momentum of the ions is transmitted to the neighboring fluid and electroosmotic flow is established. Stern and diffuse layers are generally assumed separated by a shear surface. Unlike pressurized flows, electroosmotic flows have a Plug-like velocity profile [1-3].

As some applications of electroosmotic flow, lab-on-a-chip bio-sensing systems [4-5], drug delivery [6-7], microchannel plate electroosmotic pump [8-9], flow injection analysis and pumping of liquid propellants for micro-thrusters can be mentioned [10-12]. The wide range of electroosmotic flow applications has made a large number of researchers interested in the topic, and different methods have been implemented by researchers to resolve it. Computational fluid dynamics (CFD) is one of these methods which Lattice-Boltzmann method, Finite volume method, Finite element method and Finite difference method are some of its subsets [13-18]. Semi-analytical methods like Homotopy perturbation method and Reconstruction of Variational Iteration Method are the other resolutions [19-20]. Molecular Simulation methods like Molecular Dynamics and Monte Carlo are also employed in electroosmotic flow investigations [1, 21, 22]. Among these approaches, Molecular Dynamics simulation method is used in our study. Researchers have focused on various elements that can affect electroosmotic flow such as: size and valence of ions, PH of solution, surface charge density, charge type and temperature of the wall [23-26]. As a matter of interest, in this work the main focus has been put on valence and reverse flow caused by high wall charges. Following studies are some of the previous works that have been mostly concerned about valence and reverse flow phenomenon. Some researchers studied the impact of either mono or multivalent ions on electroosmotic velocity. Rezaei et al. [1] studied surface charge density effects on the electroosmotic flow in a nanochannel filled with NaCl (monovalent ions). They observed that when the surface charge density rises, both electroosmotic flow velocity and EDL layer size increase. Prakash et al. [22] examined electrokinetic transport of monovalent and divalent cations in silica nanochannels.

According to their findings as divalent cations are added to NaCl solution, with the system being electrically neutral, maximum electroosmotic velocity is increased up to two-fold. Zambrano et al. [27] published an article studying the effect of divalent counter-ions on controlling the electroosmotic transport in nanochannels. Results showed that increased divalent counter-ions in the solution leads to a

*Corresponding Author Email: *m.kalteh@gu.ac.ir*
Tel.: +989112346354; Note. This manuscript was submitted on May 23, 2022; approved on September 15, 2022; published online March 12, 2023.

	Nomenclature		
	Lower case		**Upper case**
m	Mass of each particle	E	Applied electrical field
q	Charges of atoms	F	Force
q_{eq}	Equivalent charge	LJ	Lennard-Jones
r	Separation distance between two particles	N_{atm}	Number of atoms
$r_{Cut\ off}$	Cutoff radius	T	Absolute temperature in Kelvin
t	Time step	V_m	The steady-state velocity of the macroion
v	Velocity	V_{LJ}	The Lennard-Jones interionic potential
	Greek Symbols	$V_{Coulomb}$	The Coulomb potential
ε	Depth of the potential well		**constants**
μ	Electrophoretic motion	k_B	Boltzmann constant
σ	LJ distance size	ϵ_0	The vacuum permittivity

rise in electroosmotic velocity of the EDL layer, followed by an increase in the electroosmotic velocity of the fluid.

Moving on to reverse flow, Celebi et al. [28] analyzed intermediate and flow reversal regimes in electroosmotic transport. Several results were concluded: the increase in electroosmotic velocity as surface charge density increases in Debye–Hückel flow regime, decline in electroosmotic velocity with rising the surface charge density in intermediate flow regime and even more plunge in velocity as the surface charge density is added in reversal flow regime which leads to reversed direction of flow. The reversal flow has also appeared in Qiao and Narayana [29] and Lorenz et al. [30] studies.

In the previous works, the reverse flow of electroosmotic motion has been studied and in some other studies the presence of a divalent ion (like Mg) in an aqueous solution has been covered regardless to its impact on the reverse flow. Therefore, the aim of this article is to study electroosmotic motion of an aqueous solution containing Mg^{++} ions and to evaluate the possibility of reversed flow. The simulation is performed in various surface charge densities and particle numbers, followed by comparing the results. This is achieved using Molecular Dynamic simulations method.

MATERIALS AND METHODS

The simulation system includes two parallel silicon walls which are filled with the solution of water, Na, Cl and Mg ions. The channel walls, having 6 nm distance between, are made up of silicon atoms with FCC structure. Here, periodic boundary conditions along x and z directions are utilized. The simulation box dimensions are 45×180×60 Å, which is three times as wide as channel's height in order to reduce the electrostatic interactions of the periodic boundaries in y direction.

Inner layer of each wall includes 198 silicon atoms with negative charge which provide the required surface charge. It should be noted that outer layers are electrically neutral. The space between the walls is filled with 4361 water molecules. The electrolyte solution consists of 307 Na, Cl and Mg ions which are scattered randomly among water molecules. The number of Na, Cl and Mg ions are selected in a way that system remains electrically neutral. Figure 1 illustrates the geometry before the simulation begins.

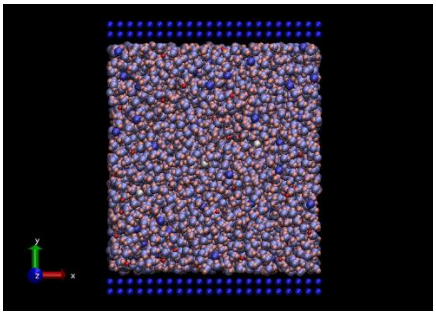

Fig. 1. Initial state schematic view of the channel

To simulate water molecules, SPC model has been used [31]. For the potential between ions, Lennard-Jones Model is used:

$$V_{LJ} = 4\varepsilon_{ij}\left[\left(\frac{\sigma_{ij}}{r}\right)^{12} - \left(\frac{\sigma_{ij}}{r}\right)^{6}\right] \quad r < r_{Cutoff} \tag{1}$$

In this equation, r represents the distance between i and j molecules. ε is energy parameter which indicates the depth of potential well and σ is the length parameter which shows molecular distance, when potential function crosses zero potential line [1].

The cut off diameter is 11 Å and the Lennard-Jones parameters are listed in Table 1.

Table 1
Lennard Jones constant parameters [1 ,25].

	ε (kCal/mole)	σ (A)
H-H	0	0
O-O	0.155	3.17
Na-Na	0.0148	2.58
Cl-Cl	0.106	4.45
Si-Si	0.584	3.39
Mg-Mg	0.874415	1.4

Lennard-Jones parameters for other chemical bonds are calculated as [1]:

$$\varepsilon_{ij} = \sqrt{\varepsilon_{ii} \cdot \varepsilon_{jj}} \quad (2)$$

$$\sigma_{ij} = \sqrt{\sigma_{ii} \cdot \sigma_{jj}} \quad (3)$$

Long-range electrostatic intermolecular interactions are enforced by Coulomb potential, the equation of which is [1]:

$$V_{Coulomb}(\mathrm{r}) = \frac{1}{4\pi\epsilon_0}\frac{q_i q_j}{r} \quad (4)$$

q_i is the atom i's charge and ϵ_0 is the vacuum permittivity. To accelerate solving the long-range electrostatic intermolecular interactions, PPPM algorithm is used with the maximum tolerance of 10^{-4}. NVT canonical ensemble (Nose-Hoover thermostat) and the temperature of 300K is also employed.2 Verlet method is applied for velocity calculations using Newton's second law integration. Below are the equations to find the particles position and velocity using this method [1]:

$$r(t+\delta t) = r(t) + v(t)\delta t + \frac{F(t)}{m}\frac{\delta t^2}{2} \quad (5)$$

$$v(t+\delta t) = v(t) + \frac{1}{2}\left[\frac{F(t)+F(t+\delta t)}{m}\right]\delta t \quad (6)$$

where r is the position, v is the velocity, F is applied force and m is the mass of each particle. δt is the time period that is considered to be 2 femtoseconds here. The initial velocity of each particle is formulated as following [1]:

$$\frac{1}{N_{atm}}\sum_{i=1}^{N_{atm}}\frac{1}{2}m|v_i^2| = \frac{3}{2}k_B T \quad (7)$$

where K_B is Boltzmann constant, T is the temperature in Kelvins and N_{Atom} is the number of atoms in the system.

Initially, the simulation is run for 1000000 time steps (equal to 2 ns) without any applied external force. Then, applying a 0.55 V/nm external electric field to the system, the simulation is continued for about 15000000 more time steps (equal to 30 ns). All simulations are done by LAMMPS software.

RESULTS AND DISCUSSION

In this section, the simulation results of electroosmotic motion of water and Na, Cl and Mg ions inside a silicon nano-channel with different surface charge densities is presented. To do this, first of all, the current results are validated with comparing them to the existing ones.

Validation

The validation here is carried out in several stages, two of which will be described in the following to keep it brief. First, water molecules are modelled by Molecular Dynamics and are validated by existing studies (Orsi [32]). Then, water-NaCl solution is modelled and validated via a comparison by Sanchez et al. [33]. In the next stage, water flow and water-NaCl inside a nano-channel are simulated in the same way. Considering the existing studies (Prakash et al. [22] and Pital et al. [34]), results show an adequate validity. Next, the electroosmotic flow of water with Na, Cl and Mg ions inside a silicon nanochannel is simulated and the results are confirmed by Prakash's work [22].

The velocity profile is presented in Figure 2 in which the number of Cl, Na and Mg equal to 65, 105 and 0, respectively.

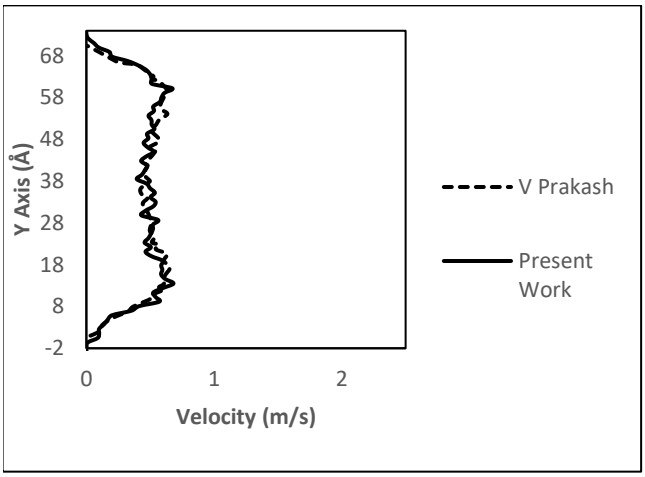

Fig. 2. Velocity comparison between present results and Prakash's work, Na=105, Cl=65, Mg=0.

The number of these ions in Figure 3 are 91, 27 and 52 in the same order. Looking thoroughly into these results, it can be seen that the obtained results show remarkable agreement with Prakash's [22] findings.

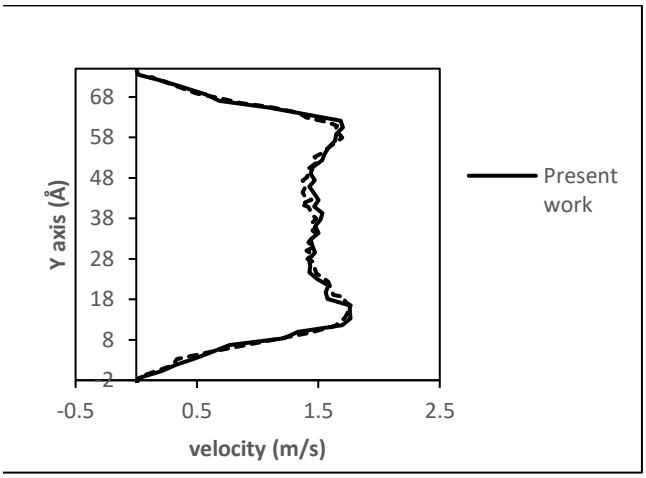

Fig. 3. Velocity comparison between present results and Prakash's work, Na=27, Cl=91, Mg=52.

RESULTS

After the validation of the modelling, the achieved results of the present work are discussed in the following. Basic

model has a surface charge density of -0.1745 C/m^2 and number of the ions are Na^+ =80, Mg^{++} =60 and Cl^- =167.

Figure 4 depicts changes in ion densities across the channel. It is observed that Na ions keep closer to the walls. As a hypothesis introduced by Prakash et al. [22], during electrostatic interactions between ions and water, ions are considered to be hydration spheres rather than individual spots. Since ionic radius of Na is more than Mg's and the fact that Mg is bivalent and Na is monovalent, applied force to water molecules by Mg is more than applied force by Na. Therefore, by moving Mg ions, more water molecules are made move.

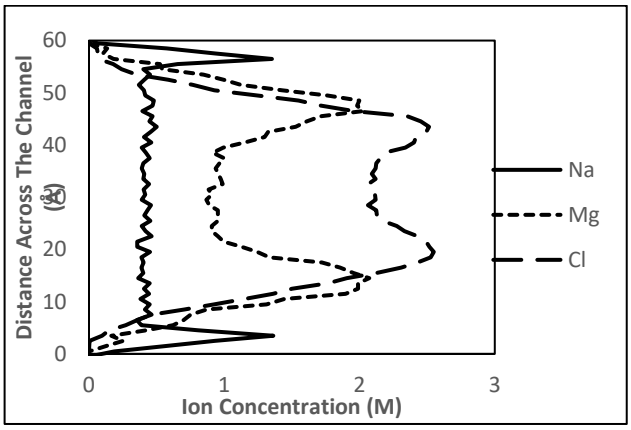

Fig. 4. Changes in ion densities versus the distance across the channel.

Figure 5 sets out average electroosmotic velocity changes by surface charge density variations with and without Mg^{++} ion in the solution. The first thing that stands out is that presence of Mg^{++} ion causes up to 31% (15 m/s) growth in average electroosmotic velocity. This is because, as Mg amount increases, Na must be decreased to keep the system electrically neutral. As it was already mentioned, Mg ions have higher hydration radius than Na. Consequently, Mg ions are surrounded by more water particles than Na. Applying electrical field, Mg ion is capable of making more water particles moving than Na. So higher electroosmotic velocity will be established.

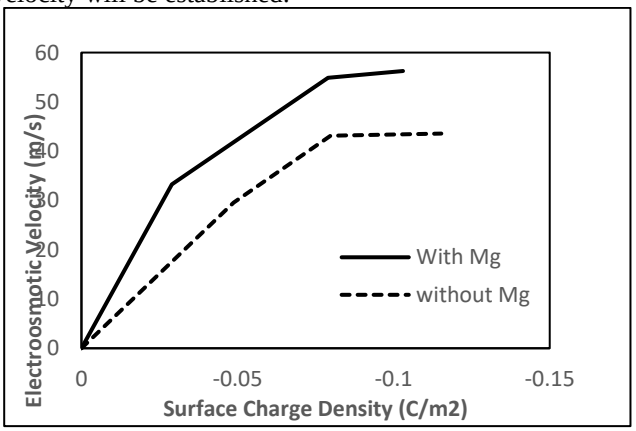

Fig. 5. Comparison between changes of average electroosmotic velocity versus surface charge density variations with and without Mg++ ions.

Figures 6 and 7 illustrate variations in the electroosmotic velocity profile across the channel and the average axial electroosmotic velocity as surface charge density changes, respectively. It can be seen that changes in the surface charge density have a profound effect on the electroosmotic velocity.

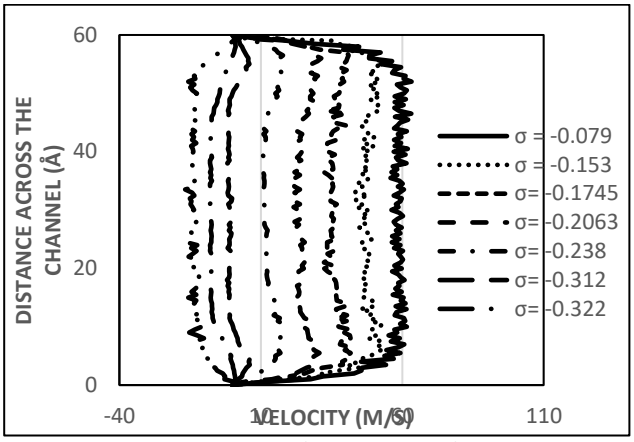

Fig. 6. Electroosmotic velocity profile in various surface charge densities.

Looking at the Figure 7, in lower surface charge densities, which Debye–Hückel flow regime rules, any increase in surface charge density leads to a rise in electroosmotic velocity (an increase in surface charge density from 0 to -0.103 C/m^2 leads to rise in average electroosmotic velocity from 0 to 57 m/s). In the intermediate flow regimes, increase in surface charge density results in a drop in electroosmotic velocity. The dual effect of electrical charge of the walls on electroosmotic motion explains this phenomenon. The electrical charge of the walls acts as both a resistor to positive ion movement and the main factor to build the EDL layer.

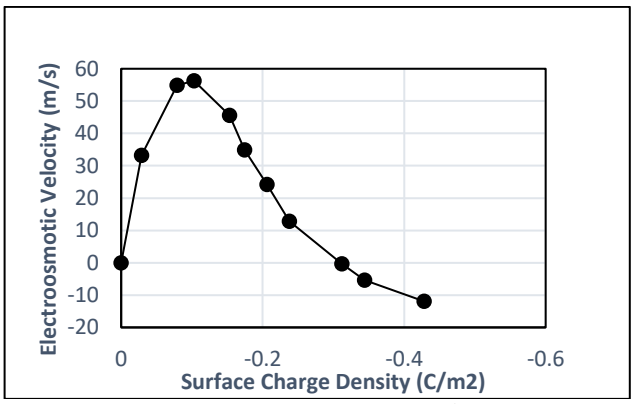

Fig. 7. Average electroosmotic velocity versus surface charge density variations.

As average velocity reaches to a maximum level (which is the boundary between Debye–Hückel and intermediate flow regimes), the thickness of EDL layer increases and a risen electroosmotic velocity is resulted. However, as the surface charge density increases, the resistance role of the wall's electrical charge against the movement of positive ions acts

more powerful, leading to a reduced electroosmotic velocity (an increase in surface charge density from -0.103 C/m^2 to -0.3 C/m^2 leads to reduce in average electroosmotic velocity from 57 to 0 m/s).

It is also observed that excessive increases in surface charge density leads to a reversed flow in the channel (an increase in surface charge density from -0.3 C/m^2 to -0.428 C/m^2 leads to rise in average reverse electroosmotic velocity from 0 to -12 m/s). Reversed flow happens when charge inversion phenomenon occurs [1]. Here, the charge inversion phenomenon occurs when the total charge of positive Mg and Na ions, that have been absorbed to Stern sublayer in the EDL, exceeds the negative charge of the wall. Consequently, the density of Cl ions goes beyond Na and Mg's in the inner flow. In other words, the wall and the Stern layer form a new layer with positive surface charge. Then Cl ions create a new EDL layer (the second EDL layer) and inner solution is positively charged. Applying an electrical field, Cl ions of the second EDL layer move in the opposite direction, so a reversed flow is formed.

CONCLUSION

In this study, the electroosmotic motion of water and Na, Cl and Mg ions inside a silicon nano-channel with different surface charge densities was examined using Molecular Dynamics simulations. The relation between electroosmotic flow and surface charge density was evaluated. Changes in the velocity profile were observed due to variations in surface charge density. According to the results, as surface charge density within Debye–Hückel flow regime increases, firstly, the velocity of electroosmotic flow rises from 0 to 57 m/s. Reaching to a peak, it then starts to fall from 57 m/s to 0. The peak point when the velocity starts to fall is when the flow regime turns from Debye–Hückel to intermediate. It was also witnessed that further increase in surface charge density can lead to a 12 m/s-fast reversed flow, which is owing to charge inversion. Finally, the effect of added Mg ions to the solution was demonstrated. It was also seen that these added ions result in an increase in average electroosmotic velocity up to 31%. Including trivalent ions and their impact on reverse flow could be future possibilities to expand this study.

Conflict of interest

The authors declare that they have no conflict of interest.

REFERENCES

[1] Rezaei M, Azimian AR, Semiromi DT. The surface charge density effect on the electro-osmotic flow in a nanochannel: a molecular dynamics study. Heat and Mass Transfer. 2015 May;51(5):661-70 .

[2] Kang Y, Li D. Electrokinetic motion of particles and cells in microchannels. Microfluidics and nanofluidics. 2009 Apr;6(4):431-60.

[3] Zhu J, Hu G, Xuan X. Electrokinetic particle entry into microchannels. Electrophoresis. 2012 Mar;33(6):916-22.

[4] Jamshaid T, Neto ET, Eissa MM, Zine N, Kunita MH, El-Salhi AE, Elaissari A. Magnetic particles: From preparation to lab-on-a-chip, biosensors, microsystems and microfluidics applications. TrAC Trends in Analytical Chemistry. 2016 May 1;79:344-62.

[5] Estevez MC, Alvarez M, Lechuga LM. Integrated optical devices for lab-on-a-chip biosensing applications. Laser & Photonics Reviews. 2012 Jul 16;6(4):463-87.

[6] Prakash J, Ramesh K, Tripathi D, Kumar R. Numerical simulation of heat transfer in blood flow altered by electroosmosis through tapered micro-vessels. Microvascular Research. 2018 Jul 1;118:162-72.

[7] Song Y, Chen P, Chung MT, Nidetz R, Park Y, Liu Z, McHugh W, Cornell TT, Fu J, Kurabayashi K. AC electroosmosis-enhanced nanoplasmofluidic detection of ultralow-concentration cytokine. Nano letters. 2017 Apr 12;17(4):2374-80.

[8] Wang X, Cheng C, Wang S, Liu S. Electroosmotic pumps and their applications in microfluidic systems. Microfluidics and nanofluidics. 2009 Feb;6(2):145-62.

[9] Cao Z, Yuan L, Liu YF, Yao S, Yobas L. Microchannel plate electro-osmotic pump. Microfluidics and nanofluidics. 2012 Sep;13(2):279-88 .

[10] Bonome EL, Cecconi F, Chinappi M. Electroosmotic flow through an $$\alpha $$ α-hemolysin nanopore. Microfluidics and Nanofluidics. 2017 May;21(5):1-9.

[11] Dasgupta PK, Liu S. Electroosmosis: a reliable fluid propulsion system for flow injection analysis. Analytical Chemistry. 1994 Jun 1;66(11):1792-8.

[12] Patel KD, Bartsch MS, McCrink MH, Olsen JS, Mosier BP, Crocker RW. Electrokinetic pumping of liquid propellants for small satellite microthruster applications. Sensors and Actuators B: Chemical. 2008 Jun 16;132(2):461-70.

[13] Yang SC, Sheu TW. Analysis of electro-osmotic flow by lattice Boltzmann simulation and Helmholtz-Smoluchowski formula. Numerical Heat Transfer, Part B: Fundamentals. 2020 Sep 18;79(3):130-49.

[14] Saravani MS, Kalteh M. Heat transfer investigation of combined electroosmotic/pressure driven nanofluid flow in a microchannel: Effect of heterogeneous surface potential and slip boundary condition. European Journal of Mechanics-B/Fluids. 2020 Mar 1;80:13-25.

[15] De S, Gopmandal PP, Kumar B, Sinha RK. Effect of hydrophobic patch on the modulation of electroosmotic flow and ion selectivity through nanochannel. Applied Mathematical Modelling. 2020 Nov 1;87:488-500.

[16] Bag N, Bhattacharyya S, Gopmandal PP, Ohshima H. Electroosmotic flow reversal and ion selectivity in a

soft nanochannel. Colloid and Polymer Science. 2018 May;296(5):849-59.

[17] Fuhrmann J, Guhlke C, Linke A, Merdon C, Müller R. Induced charge electroosmotic flow with finite ion size and solvation effects. Electrochimica Acta. 2019 Sep 10;317:778-85.

[18] Liang P, Wang S, Zhao M. Numerical study of rotating electroosmotic flow of Oldroyd-B fluid in a microchannel with slip boundary condition. Chinese Journal of Physics. 2020 Jun 1;65:459-71.

[19] Jalili P, Ganji DD, Jalili B, Ganji DR. Evaluation of electro-osmotic flow in a nanochannel via semi-analytical method. Thermal Science. 2012;16(5):1297-302.

[20] Jalili P, Imani AA, Jalili B, Firouzi F, Ganji DD, Rokni HB. Assessment of the electroosmotic flow through a nano tube. ChemXpress 2014. 3. 11-15.

[21] Ocampo LP, Weiss LB, Jardat M, Likos CN, Dahirel V. Electroosmotic Flow Induced Lift Forces on Polymer Chains in Nanochannels. ACS Polymers Au. 2022 Aug 8;2(4):245.

[22] Prakash S, Zambrano HA, Rangharajan KK, Rosenthal-Kim E, Vasquez N, Conlisk AT. Electrokinetic transport of monovalent and divalent cations in silica nanochannels. Microfluidics and Nanofluidics. 2016 Jan;20(1):1-8.

[23] Tran TH, Phan GT, Luc HT, Nguyen PT, Hoang H. Molecular dynamics simulations on aqueous solution confined in charged nanochannels: asymmetric effect of surface charge. Molecular Simulation. 2020 Jul 2;46(10):796-804.

[24] Rezaei M, Azimian AR, Toghraie D. Molecular dynamics study of an electro-kinetic fluid transport in a charged nanochannel based on the role of the stern layer. Physica A: Statistical Mechanics and its Applications. 2015 May 15;426:25-34.

[25] Celebi AT, Beskok A. Molecular and continuum transport perspectives on electroosmotic slip flows. The Journal of Physical Chemistry C. 2018 Apr 16;122(17):9699-709.

[26] Li J, Peng R, Li D. Effects of ion size, ion valence and pH of electrolyte solutions on EOF velocity in single nanochannels. Analytica Chimica Acta. 2019 Jun 20;1059:68-79 .

[27] Zambrano H, Conlisk T. Controlling the electroosmotic transport in nanochannels: effect of divalent counter-ions. In51st AIAA Aerospace Sciences Meeting including the New Horizons Forum and Aerospace Exposition 2013 Jan (p. 1115).

[28] Celebi AT, Cetin B, Beskok A. Molecular and continuum perspectives on intermediate and flow reversal regimes in electroosmotic transport. The Journal of Physical Chemistry C. 2019 May 13;123(22):14024-35.

[29] Qiao R, Aluru NR. Charge inversion and flow reversal in a nanochannel electro-osmotic flow. Physical review letters. 2004 May 10;92(19):198301 .

[30] Lorenz CD, Travesset A. Charge inversion of divalent ionic solutions in silica channels. Physical Review E. 2007 Jun 13;75(6):061202.

[31] Mark P, Nilsson L. Structure and dynamics of the TIP3P, SPC, and SPC/E water models at 298 K. The Journal of Physical Chemistry A. 2001 Nov 1;105(43):9954-60 .

[32] Orsi M. Comparative assessment of the ELBA coarse-grained model for water. Molecular Physics. 2014 Jun 3;112(11):1566-76.

[33] Sanchez MC, Gujt J, Sokolowski S, Pizio O. Effects of ion concentration and solvent composition on the properties of water-methanol solutions of NaCl. NPT molecular dynamics computer simulation results. Condensed Matter Physics. 2018;21(2).

[34] Kucaba-Piętal A, Walenta Z, Peradzyński Z. Molecular dynamics computer simulation of water flows in nanochannels. Bulletin of the Polish Academy of Sciences: Technical Sciences. 2009:55-61.